talenta PUBLISHER

Eco Chemical Engineering Journal

Journal homepage: https://talenta.usu.ac.id/EcoChe

Metal Organic Frameworks and Their Derivatives as Catalysts for Converting Biomass, Lipid and Waste Plastic Feedstocks into Sustainable Aviation Fuel: A Mini Review of Experimental Studies (2017–2026)

Dikki Miswanda*[1], Devi Lestari[1], Imas Masriah[1], Juli Novita Sari[2], Amru Daulay[3]

[1] *Industrial Chemical Engineering Technology, Politeknik Negeri Medan, Medan, Indonesia*

[2] *Department of Chemistry, Faculty of Vocational Studies, Universitas Sumatera Utara, Jalan Tri Dharma Kampus USU, Padang Bulan, Medan, 20155, Indonesia*

[3] *Research Center for Mineral Technology, National Research and Innovation Agency (BRIN), Jl. Ir. Sutami, Km. 15, Tanjung Bintang, South Lampung, Lampung Province, Indonesia*

*Corresponding Author: dikkimiswanda@polmed.ac.id

Article info

Article history:
Received 8 October 2026
Revised 15 October 2026
Accepted 20 October 2026
Available online xxx

E–ISSN:
P–ISSN:

How to cite:
D. Miswanda, D. Lestari, I. Masriah, J. N. Sari, A. Daulay, "Metal–Organic Frameworks and Their Derivatives as Catalysts for Converting Biomass, Lipid and Waste–Plastic Feedstocks into Sustainable Aviation Fuel: A Mini–Review of Experimental Studies (2017–2026)," Eco Chemical Engineering Journal, Vol. 1 No. 1.

This work is licensed under a Creative Commons Attribution–ShareAlike 4.0 International.

http://doi.org/10.26594/register.v6i1.idarticle

Abstract

Sustainable aviation fuel (SAF) is the main near term option for decarbonising aviation, but most conversion routes require catalysts that combine metal, acid and/or base functions while tolerating water, coke and bulky molecules. Metal organic frameworks (MOFs) offer tunable nodes, linkers and pores, and can also be pyrolysed into highly dispersed metal/carbon or metal–oxide catalysts. This mini review maps 29 experimental studies published between 2017 and 2026 that used pristine MOFs, MOF hybrids or MOF derived materials to produce SAF range hydrocarbons or their precursors. Five routes were identified: C–C coupling of furanic platform molecules (9 studies), deoxygenation and cracking of lipids and fatty acid methyl esters (10), hydrogenation/hydrodeoxygenation of cyclic oxygenates, terpenes and lignin models (4), upcycling of waste plastics (4) and Fischer Tropsch synthesis (2). MOF derived materials dominated (17 studies), followed by pristine MOFs (6) and MOF hybrids (6). Best case performances were high, including ≈100% furfural conversion and adduct selectivity over defect engineered UiO–66(Zr), 82–84% jet range selectivity from methyl palmitate over Ni–MOF–based catalysts, 96% p-menthane over MIL–101–SO_3H^+ Pd/C, and 75.2% C8–C16 selectivity in Fischer-Tropsch synthesis. Standardised reporting, long duration tests with real feedstocks, fair benchmarking, and scalable MOF synthesis are key priorities.

Keywords: Sustainable aviation fuel, Bio jet fuel, Metal organic frameworks, MOF derived catalysts, Aldol condensation

1. Introduction

Aviation is one of the hardest transport sectors to decarbonise. Battery electric and hydrogen propulsion remain constrained by energy density, weight and refuelling time for medium and long haul flights, so liquid hydrocarbon fuels will continue to power most commercial aircraft for decades [1]. Aviation accounts for roughly 2% of anthropogenic greenhouse gas emissions and 11–12% of transport related CO_2 emissions [2]. The International Air Transport Association (IATA) has committed the industry to net zero carbon emissions by 2050, a target that has been associated with a demand for biomass derived sustainable aviation fuel (SAF) of the order of 449 billion litres per year [3]. Analyses by the International Civil Aviation Organization (ICAO) summarised by Qi et al. indicate that, in 2050, SAF could provide an additional 56% reduction in net lifecycle

CO_2 beyond the 27% expected from technology and operational improvements [4], whereas current SAF output (about 0.2 Mt) is two orders of magnitude below the ~28 Mt projected for 2050 [5].

SAF must be a drop in fuel: its hydrocarbons must fall predominantly in the C_8–C_{16} range and combine appropriate proportions of *n*-paraffins, iso-paraffins, cycloalkanes and aromatics to meet density, freezing-point, flash-point and energy content requirements [6], [7]. Converting renewable feedstocks into such molecules usually requires two families of reactions. Short platform molecules (C_5–C_6 furanics, ketones) must be lengthened by C–C coupling before being deoxygenated, whereas long chain lipids (C_{16}–C_{18}) must be deoxygenated and partially cracked. Cyclic oxygenates, terpenes, lignin fragments and oxygenated plastics additionally require hydrogenation and selective C–O cleavage without ring opening, while syngas derived Fischer Tropsch (FT) products must be steered away from the statistical Anderson–Schulz–Flory distribution, which limits the C_8–C_{16} fraction of conventional FT synthesis to about 41% [7]. Across these routes, the catalyst must place metal, acid and/or base functions in the right proportion and proximity, tolerate water and oxygenated by products, admit bulky molecules and resist sintering, leaching and coke formation [3], [8].

Metal organic frameworks (MOFs), crystalline networks of metal ions or clusters connected by organic linkers, are attractive in this context because their nodes, linkers, pore sizes and defect densities can be tuned with a precision that is difficult to achieve with conventional oxides or zeolites [9]. MOFs can act as catalysts in their own right (for example, through open metal sites, μ_3–OH groups on Zr_6 clusters, or grafted –SO_3H groups), as hosts for encapsulated active species, or as sacrificial precursors that are pyrolysed into highly dispersed metal, metal phosphide or metal oxide nanoparticles embedded in carbon or oxide matrices [8], [10], [11]. Their principal weaknesses are equally well known: limited hydrothermal and thermal stability, micropores that restrict bulky reactants and products, and synthesis costs that complicate scale up [9], [12].

Research on MOF based catalysts for SAF has grown rapidly, but it is scattered across very different feedstocks (furfural, lipids, terpenes, lignin, plastics, syngas) and reported in heterogeneous formats. This mini review maps a body of 29 experimental studies published between 2017 and 2026 in which pristine MOFs, MOF hybrids or MOF derived materials were used to produce SAF range hydrocarbons or their direct precursors. The aims are (i) to chart which feedstocks, conversion routes and catalyst design strategies have been investigated; (ii) to compare the reported operating conditions, performance and stability; and (iii) to identify the evidence gaps that currently limit the translation of MOF catalysis to SAF production.

2. MOF based catalytic routes to sustainable aviation fuel

The 29 studies fall into five conversion routes (Table 1, Figure 1a): C–C coupling of furanic platform molecules (9 studies), deoxygenation and cracking of lipids and fatty acid methyl esters (FAMEs) (10), hydrogenation and hydrodeoxygenation (HDO) of cyclic oxygenates, terpenes and lignin derived compounds (4), chemical upcycling of waste plastics (4), and Fischer Tropsch synthesis from syngas (2). With respect to the role played by the framework, MOF derived materials obtained by pyrolysis or calcination dominate (17 studies), followed by pristine MOFs used as catalysts (6) and MOF hybrids or composites in which the framework is supported on, or encapsulates, another phase (6). The corpus is strongly weighted towards recent work: 20 of the 29 studies appeared in volumes dated 2023–2026, and 10 in 2026 alone (Figure 1b).

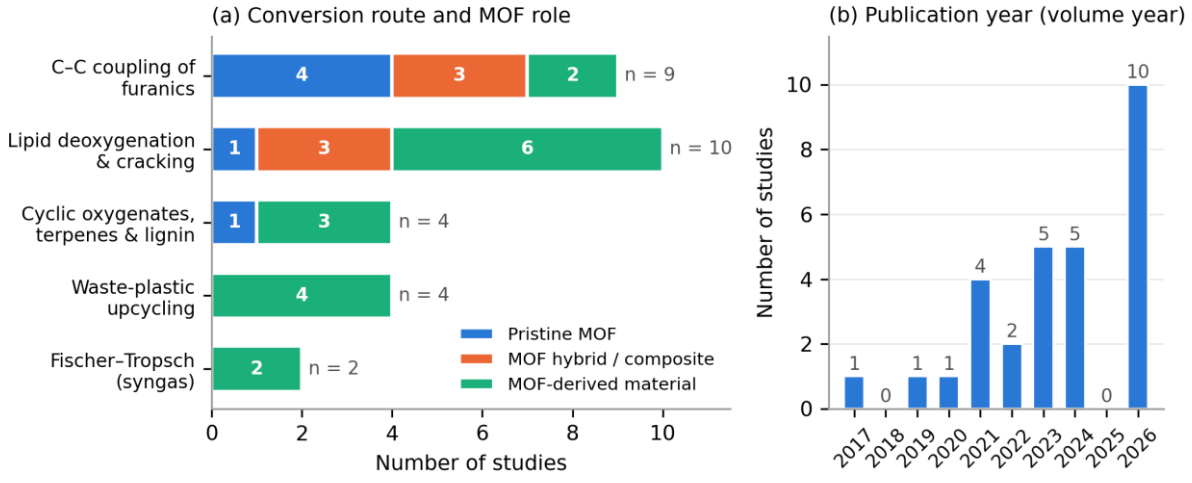


Figure 1. Evidence map of the 29 studies reviewed. (a) Number of studies per conversion route. (b) Number of studies per publication (volume) year.

Table 1. Evidence map of the 29 experimental studies on MOF based catalysts for SAF range hydrocarbons and their precursors, grouped by conversion route

No.	Ref.	Feedstock	Catalyst (MOF precursor / architecture)	Role of MOF	Main product
C–C coupling of furanic platform molecules					
1	[11]	HMF + acetone	Al exchanged DTP encapsulated in ZIF–8 ($Al_{0.66}$–DTP@ZIF–8)	Hybrid	C_9/C_{15} aldol adducts
2	[13]	Furfural + MIBK (solvent free)	Cs on ZrO_2/C from GO/UiO–66, octyl–grafted	Derived	C_{11} branched adduct (FMIBK)
3	[10]	Furfural + MIBK	Defective UiO–66(Zr), formic acid modulated	Pristine	C_{11} adduct (FuMe)
4	[14]	Furfural + MIBK	Zr–MOF–808 grown on MCM–41 / SBA–15	Hybrid	FuMe
5	[5]	Furfural + acetone; cyclopentanone	MOF–808 extrudates (vs. hydrotalcite, doped alumina)	Pristine (shaped)	C_8/C_{13} adducts
6	[15]	Furfural + MIBK	UiO–66(Zr) modulated with FA, TFA or HCl	Pristine	FuMe
7	[9]	Furfural + MIBK	Zr–MOFs (UiO–66, MOF–808, DUT–52, DUT–84)@SBA–15	Hybrid	FuMe
8	[1]	Furfural + cyclic ketones	UiO–66(Zr)–HCl (defective)	Pristine	C_{10}–C_{12} cycloalkane precursors
9	[16]	Furfural + acetone (one pot)	Ni_2P@C from Ni–BTC, ethylenediamine–grafted	Derived	C_8–C_{13} alkanes
Deoxygenation and cracking of lipid feedstocks					
10	[17]	Palmitic and lauric acids	0.5 wt% Pt/ZIF–67 membrane/zeolite 5A beads	Hybrid	C_{15}, C_{11} alkanes
11	[18]	Methyl palmitate	Ni–BTC nanosheets in MCM–41 (2.5 wt% Ni)	Hybrid	C_8–C_{16} hydrocarbons
12	[6]	Methyl palmitate	Ni–DOBDC (hydroxylated BDC Ni–MOF)	Pristine	C_8–C_{16} hydrocarbons
13	[8]	Methyl palmitate; microalgal biodiesel	Ni nanoparticles on C from Ni–BDC (600 °C)	Derived	C_8–C_{16} hydrocarbons
14	[19]	Methyl palmitate; microalgal biodiesel	Ni@C from Ni–BTC (500 °C)	Derived	C_8–C_{16} hydrocarbons
15	[20]	Oleic acid	Pt–Ni on hierarchical γ–Al_2O_3 from Al–MOF	Derived	C_8–C_{17} alkanes
16	[4]	Methyl palmitate; microalgal biodiesel	Co–Mo–Ni from ion–exchanged Ni–BDC–NH_2	Derived	C_8–C_{16} hydrocarbons
17	[2]	Coconut oil	Ni on ZIF–67–derived Co oxide (10Ni/Co–C)	Derived	C_{11}–C_{17} paraffins
18	[21]	Waste cooking oil	Cu–2–methylimidazole MOF/K_2O, treated at 500 °C	Derived	Gasoline/kerosene/diesel mix
19	[22]	Microalgal lipids (direct)	Peroxopolytungstate in MIL–100(Cr) (PW_4@MIL–100(Cr))	Hybrid	C_{14}–C_{24} alkanes
Hydrogenation/HDO of cyclic oxygenates, terpenes and lignin models					
20	[3]	Cineoles, eucalyptus oil, 2,5–DMF, C_{11}–C_{26} multifuranics	MIL–101–SO_3H + Pd/C (mechanical mixture)	Pristine (tandem)	p–Menthane; single component n n alkanes
21	[23]	Lignin dimer models; monophenols	NiLa@C from Ni/La–BTC	Derived	Cycloalkanes + cyclohexanol
22	[24]	Heavy turpentine (sesquiterpenes)	Ni@C/rGO from Ni–MOF–74/GO	Derived	Hydrogenated sesquiterpenes (high density fuel)
23	[25]	α–Pinene (solvent free)	Ni on g–C_3N_4 from Ni–MOF/g–C_3N_4	Derived	cis–Pinane
Chemical upcycling of waste plastics					
24	[26]	Municipal plastic mix (HDPE, LDPE, PP, PS, PVC, PET)	Cu/CuO_x@C from MIL–53(Cu) on zeolite Y	Derived	Gasoline, jet and diesel cuts
25	[12]	Waste polycarbonate	NiCo/C from Co–terephthalate MOF	Derived	Cycloalkanes (mainly cyclohexane)

No.	Ref.	Feedstock	Catalyst (MOF precursor / architecture)	Role of MOF	Main product
26	[27]	Municipal plastic mix	Cu/CuO_x@C from MIL–53(Cu) on zeolite Y	Derived	Gasoline, jet and diesel cuts
27	[28]	Real PC wastes incl. compact discs	MoCo/NiC from Ni–terephthalate MOF	Derived	Jet range cycloalkanes
Fischer Tropsch synthesis (syngas)					
28	[29]	Syngas (H_2/CO 1.6–2)	Ru–Co@C(ZIF–67–derived)@Void@CeO_2	Derived	C_{5+}, C_8–C_{16}
29	[7]	Syngas (H_2/CO = 2)	Co@SiO_2 from APTES–infused ZIF–67 + ZSM–5	Derived	C_8–C_{16} (iso paraffin rich)

Abbreviations: BDC, terephthalate; BTC, 1,3,5–benzenetricarboxylate; DOBDC, 2,5–dioxidoterephthalate; DTP, dodecatungstophosphoric acid; DMF, 2,5–dimethylfuran; FuMe, 1–(furan–2–yl)–5–methylhex–1–en–3–one; GO/rGO, (reduced) graphene oxide; HMF, 5–hydroxymethylfurfural; MIBK, methyl isobutyl ketone; PC, polycarbonate. Role of MOF: Pristine, framework used as the catalyst; Hybrid, framework supported on or hosting another phase; Derived, framework converted by pyrolysis/calcination.

2.1. C–C coupling of furanic platform molecules

Aldol condensation of furfural (FUR) or 5–hydroxymethylfurfural (HMF) with ketones is the most frequently studied MOF catalysed route in this corpus. Five of the nine studies come from a single research group and use the same model reaction, the condensation of FUR with methyl isobutyl ketone (MIBK) to the C_{11} adduct 1–(furan–2–yl)–5–methylhex–1–en–3–one (FuMe), which can be hydrodeoxygenated to branched jet–range alkanes [1], [9], [10], [14], [15].

Defect engineering of UiO–66(Zr) is the clearest design lever. Using formic acid as a synthesis modulator introduced missing–linker and missing node defects that exposed weakly Brønsted–acidic μ_3–OH groups on the Zr_6 clusters, and under optimised conditions (130 °C, 4 h, MIBK/FUR = 4) FUR conversion and FuMe selectivity both approached 100% [10]. A subsequent comparison of formic acid, trifluoroacetic acid and HCl showed that modulators with lower pK_a create more defects and, in the case of HCl, more missing–cluster defects that improve accessibility; the best HCl modulated material gave 96% conversion with 97% FuMe selectivity [15]. The same defective UiO–66(Zr)–HCl catalysed the condensation of FUR with cyclic ketones to C_{10}–C_{12} cycloalkane precursors, with 2–methylcyclohexanone giving >98% conversion and ~100% selectivity at 130 °C in 2 h, whereas cyclopentanone, cyclohexanone and 4–methylcyclohexanone suffered from self and over condensation [1].

The recurring weakness of crystalline Zr–MOFs is deactivation. Organic deposits from furfural side reactions progressively deactivated defective UiO–66(Zr) [10], and bulk MOF–808 lost activity rapidly [14]. Dispersing the MOF phase on mesoporous silica was the most consistent mitigation. Zr–MOF–808 grown on MCM–41 was about twice as active as bulk MOF–808 while containing <10% of its Zr, giving 68% conversion and 90% selectivity at a FUR:Zr mass ratio of 150, and 100% conversion and selectivity at 75; under continuous flow, mean FUR conversion was 21% for the hybrid versus 7% for the bulk MOF, which deactivated completely within 2.7 h [14]. Similarly, UiO–66@SBA–15 raised FUR conversion from 3% (bulk UiO–66) to 67% with 100% selectivity [9]. Continuous operation also helped: UiO–66(Zr)–HCl, which deactivated in batch mode, was markedly more stable in a fixed–bed flow reactor, which the authors attributed to shorter residence times and continuous removal of fouling species [1]. In the only study to use a shaped MOF in a fixed bed for an extended period, MOF–808 extrudates gave >85% conversion in the furfural–acetone condensation at 100–120 °C and remained stable for 53 h on stream, favouring the C_{13} over the C_8 adduct; however, unlike the hydrotalcite and alumina benchmarks, the MOF could not be regenerated by calcination above 200 °C [5].

Two studies explored alternative active sites. Encapsulating Al exchanged dodecatungstophosphoric acid in ZIF–8 ($Al_{0.66}$–DTP@ZIF–8) produced a stable acid catalyst for HMF–acetone condensation (98–99% HMF conversion after 10 h at 160 °C), with the small ZIF–8 aperture favouring the C_9 monomer adduct (84.1% selectivity) over the C_{15} dimer; activation energies of 65.3 and 102.1 kJ mol^{-1} for monomer and dimer formation, respectively, confirmed kinetic control [11]. At the basic end, only Cs species supported on zirconia/carbon derived from graphene–oxide/UiO–66 composites provided basic sites strong enough to activate MIBK (88.6% FMIBK yield at 130 °C, 6 h); grafting octyl groups to render the surface hydrophobic protected it from reaction water and allowed four reuse cycles [13].

The only study in this group to deliver alkanes rather than oxygenated precursors combined both steps in one pot. Ni_2P@C catalysts derived from Ni–BTC and grafted with ethylenediamine provided basic –NH_2 sites for condensation together with Lewis and Brønsted acid sites (from Ni→P electron transfer and P–OH groups) for HDO, converting furfural and acetone completely with an 86% yield of C_8–C_{13} alkanes at 230 °C and 2

MPa H_2 in 4 h, and retaining activity over five cycles [16]. A physical mixture of separately prepared basic and phosphide catalysts gave only 73%, which the authors attributed to carbon losses during intermediate handling [16].

2.2. Deoxygenation and cracking of lipid feedstocks

Ten studies addressed lipid derived feedstocks: model fatty acids (palmitic, lauric, oleic), methyl palmitate as a FAME model, microalgal biodiesel and lipids, coconut oil and waste cooking oil. Here, the MOF usually serves as a source of highly dispersed metal (mainly Ni) after pyrolysis, although three studies used the framework in intact or supported form.

A coherent line of work on Ni–MOFs illustrates how the framework has been exploited [4], [6], [8], [18], [19]. Loading Ni–BTC nanosheets inside MCM–41 increased the spacing between Ni sites (0.98 nm versus 0.20 nm in Ni nanoparticles), which was argued to ease access for methyl palmitate (0.68 nm wide); at 2.5 wt% Ni the catalyst used 75% less Ni than a conventionally impregnated 10 wt% Ni/MCM–41 yet raised the alkane yield from 23.3% to 33.9% and cut the arene yield from 22.4% to 6.5%, giving an overall jet–range yield of 53.2% under 2 MPa H_2 at 390 °C [18]. Subsequent studies replaced H_2 with CO_2 as the reaction atmosphere. Hydroxylating the terephthalate linker (Ni–DOBDC) increased the BET area from 57.6 to 901 m^2 g^{-1} and the strong acid density from 0 to 0.75 mmol g^{-1}, lifting the selectivity to jet–range hydrocarbons from 68% to 82% at 430 °C [6]. Pyrolyzing Ni–BDC at 600 °C generated Ni nanoparticles on carbon, increased strong acidity to 0.835 mmol g^{-1} and the Lewis/Brønsted ratio from 8.34 to 24.71, and gave 83.5% jet–range selectivity from methyl palmitate and 75.6% from microalgal biodiesel [8]. Pyrolysed Ni–BTC (Ni@C500) reached 71.5% selectivity at a catalyst to feed mass ratio of only 1:200, and 71.6% selectivity at 97.5% conversion with microalgal biodiesel [19]. Ion exchanging Co and Mo into Ni–BDC–NH_2 before pyrolysis created oxygen vacancies and Co→Ni→Mo electron transfer, giving 70.8–82.8% jet range selectivity at catalyst to feed ratios of 1:50–1:200 [4]. These results are internally consistent, but all were obtained in batch autoclaves at 390–460 °C, where thermal cracking contributes substantially, and none of the four CO_2 atmosphere studies reported catalyst reuse.

Other studies focused on selective decarboxylation, which yields odd numbered alkanes one carbon shorter than the parent acid. Pt (0.5 wt%) on ZIF–67 membranes grown on zeolite 5A beads gave ≥95% deoxygenation of palmitic and lauric acids in 2 h, with ~92% pentadecane and ~94% undecane selectivity under CO_2; H_2 promoted competing HDO, and esters were identified as the key intermediates [17]. Hierarchical γ–Al_2O_3 derived from an Al–MOF (BET area 266.8 m^2 g^{-1}) supported Pt–Ni catalysts that converted oleic acid to C_8–C_{17} alkanes in 85.3% yield at 340 °C under 18 bar CO_2, retaining 77.4% yield after four recycles [20]. Ni supported on ZIF–67–derived Co oxide (10Ni/Co–C) converted coconut oil at 350 °C and 30 bar H_2 with a 99.0% hydrocarbon yield and 91.6% selectivity to jet range paraffins, mainly C_{11}–C_{17} via decarboxylation/decarbonylation; in reuse tests the yield fell from 97.6% to 66.8% and 56.9% in the second and third runs [2].

Two studies applied MOF based catalysts to low cost or unrefined lipids. A Cu–2–methylimidazole framework doped with K_2O and heat treated at 500 °C (which decomposed it to CuO/Cu_2O) gave an 83.9% organic liquid product yield from waste cooking oil at 400 °C under atmospheric N_2, of which 29% was in the kerosene range [21]. Peroxopolytungstate incorporated in MIL–100(Cr) converted microalgal lipids directly, without prior transesterification, at 180 °C with isopropanol as an in situ hydrogen donor; alkanes accounted for 53% of the relative GC-MS peak area, with tetracosane, eicosane and heneicosane as the dominant products [22]. Because these C_{20}–C_{24} alkanes lie above the jet fuel range, this system is better described as a renewable–diesel than a SAF route.

2.3. Hydrogenation and hydrodeoxygenation of cyclic oxygenates, terpenes and lignin derived compounds

Cyclic hydrocarbons are valued in SAF for their density and low freezing points, and four studies targeted them. The most mechanistically detailed study in the corpus used a mechanically mixed tandem catalyst of the acidic MOF MIL–101–SO_3H (BET area 2006 m^2 g^{-1}) and commercial Pd/C for the precise HDO of cyclic ethers and furanics to single component alkanes [3]. 1,4–Cineole was converted to *p*–menthane in 96% yield at 120 °C and 30 bar H_2 in 3 h without solvent; 1,8–cineole and eucalyptus oil (50 mmol scale) gave 95% and 94% isolated yields, respectively. Two stage temperature programmes (80 °C for 3 h, then 200 °C for 10 h at 40 bar H_2) converted C_{11}–C_{26} multifuranic precursors to alkanes in yields up to 98% with GC purities up to 99%, and a C_{16} precursor was processed on a 10 g scale (91% isolated yield) [3]. Control experiments were decisive: neither Pd/C alone nor Pd/C combined with sulfonate free MIL 101 converted 1,4–cineole, whereas MIL–101–SO_3H alone gave full conversion but only oligomers. Benchmark solid acids combined with Pd/C were less selective (UiO–66–SO_3H 56%, Nafion 88%, Amberlyst–15 82%, HZSM–5 52%, montmorillonite

K10 16% *p*–menthane yield), and the yields broadly tracked the ether adsorption selectivity of each acid. Adsorption microcalorimetry showed stronger binding of 2,5–dimethyltetrahydrofuran (-92.6 kJ mol^{-1}) and 2–hexanol (-83.5 kJ mol^{-1}) than of 1,5–hexadiene (-75.3 kJ mol^{-1}) or *n*–hexane (-75.0 kJ mol^{-1}), supporting a mechanism in which oxygenates are preferentially adsorbed in the MOF pores and olefinic intermediates are expelled to the separate Pd/C particles before they can oligomerise or isomerise. ^{31}P solid state NMR with trimethylphosphine and trimethylphosphine oxide probes showed that both $–SO_3H$ groups and water coordinated to open Cr^{3+} sites contribute Brønsted acidity, making the MOF water tolerant. The mixed catalyst was reused through six recoveries in the cineole reaction, with a small loss in the sixth run restored by adding 0.2 mol% fresh Pd/C [3].

Two MOF–derived Ni catalysts addressed terpene hydrogenation. Ni@C/rGO obtained by low–temperature pyrolysis of Ni–MOF–74 grown on graphene oxide stabilised 42.3 wt% Ni as 5.35 nm particles and hydrogenated heavy turpentine (mainly sesquiterpenes) with 99.8% conversion at 150 °C and 4 MPa H_2 in 140 min, outperforming 2 wt% Pd/C; the product had a density of 0.914 g mL^{-1}, a volumetric net heat of combustion of 39.44 MJ L^{-1}, a freezing point of −73 °C and a flash point of 96 °C, comparable to JP–10, and conversion remained 82.7% after ten cycles [24]. Ni–decorated graphitic carbon nitride derived from a Ni–MOF/g–C_3N_4 composite hydrogenated α–pinene under solvent free conditions at 65 °C and 1.5 MPa H_2 with >99% conversion and 98.2% selectivity to *cis*–pinane; interfacial hydrogen spillover onto the support raised the turnover frequency to 6.28 h^{-1}, 3.2 times that of Ni on carbon [25].

For lignin, NiLa@C catalysts derived from Ni/La–BTC frameworks cleaved C–O bonds in lignin dimer models and hydrogenated the fragments in one pot (240 °C, 2 MPa H_2, isopropanol). 2–Phenoxy–1–phenylethanol gave 98% ethylcyclohexane and 86% cyclohexanol, but yields fell for methoxylated dimers (58% and 45% cyclohexanol for guaiacyl and syringyl analogues), showing that methoxy removal remains the bottleneck [23]. La addition improved Ni dispersion and acidity, and the catalyst was reused five times with a slight decline [23].

2.4. Chemical upcycling of waste plastics

Four studies applied MOF–derived catalysts to plastic waste, which is not a biogenic feedstock but is increasingly considered for circular aviation fuels. Two studies upgraded polycarbonate (PC), whose bisphenol A units yield phenolics on pyrolysis. In a tandem hydropyrolysis/vapour phase HDO micro reactor (PC pyrolysed at 500 °C, HDO at 300 °C, 0.7 MPa H_2), NiCo/C derived from a Co–terephthalate MOF converted the phenolic vapours completely to cycloalkanes, with cyclohexane as the main product (55.6% selectivity), whereas only phenolics were formed without a catalyst [12]. A MoCo/NiC heterojunction catalyst built on a Ni–terephthalate derived carbon operated at a lower HDO temperature (230 °C) and H_2 pressure (0.15 MPa), giving an average cycloalkane yield of 84.5% across four real PC wastes and 86.8% (85.4% after regeneration) from waste compact discs [28]. Both studies, however, used milligram quantities of plastic, high catalyst to feed ratios (5:1 and 20:1) and yields derived from GC MS peak areas.

The other two studies used MIL–53(Cu) impregnated on zeolite Y and pyrolysed to form Cu/CuO_x clusters encapsulated in carbon, as a cracking catalyst for mixed municipal plastics (HDPE, LDPE, PP, PS, PVC, PET) in a fixed bed [26], [27]. The highest measured jet fraction yield was 48.6% at 500 °C with a low crystallinity support [26], and a response–surface model predicted up to 73.1% at 525 °C, 2.5% catalyst loading and an amorphous support [27]. The predicted optimum lies at the edge of the experimental design space, and the jet fraction was characterised by an "octane number" rather than by jet fuel specification properties, so these values cannot be compared directly with SAF requirements.

2.5. Syngas to SAF by Fischer Tropsch synthesis

Two studies used ZIF–67 as a template for Co FT catalysts. A hollow Ru–promoted Co@C(ZIF–67–derived)@Void@CeO_2 catalyst improved Co reducibility and dispersion, increasing CO conversion by 56% relative to the Ru–free catalyst at 12 bar; at 17.5 bar and $H_2/CO = 2$ (245 °C) it reached 90.3% CO conversion and 92% C_{5+} selectivity, favoured the $C_8–C_{16}$ fraction, and lost only 4.2% of its activity over 192 h on stream [29]. Co nanoparticles confined in amorphous silica derived from APTES infused ZIF–67 (Co@3Si), combined with ZSM–5 for cracking and isomerisation, achieved 75.2% $C_8–C_{16}$ selectivity (24.3% iso–paraffins), 6.3% CH_4 and 85.1% CO conversion at 240 °C and 2 MPa, and remained stable for at least 168 h [7]. These are the longest continuous stability tests in the corpus, and the bifunctional "assembly line" design, with the MOF derived metal phase growing chains and the zeolite cracking and isomerising them, clearly exceeds the ~41% statistical limit of conventional FT synthesis [7].

3. Analysis and perspectives

3.1. What the framework contributes

The corpus shows three distinct roles for MOFs, and the evidence behind each is different (Table 3). As *intact catalysts*, MOFs contributed well defined acid or base sites that could be tuned by defect engineering (UiO–66, MOF–808) or linker functionalisation (–SO_3H, –OH), and pore environments that governed selectivity through confinement (the C_9 selectivity of ZIF–8 [11]) or adsorption preference (MIL–101–SO_3H [3]). These are the studies in which the MOF structure can be most directly linked to catalytic function, but, with one exception discussed below [6], they were used in low temperature reactions (≤200 °C) and were the most prone to deactivation by fouling. As *hybrids*, MOFs were dispersed on mesoporous silica or zeolite supports, or used to host guest species, which consistently improved accessibility and stability relative to the bulk MOF [9], [14], [18], [22]. As *precursors*, MOFs served mainly as a route to small, well dispersed and often multimetallic nanoparticles embedded in N– or O–doped carbon or oxide matrices, which accounts for their use in high temperature lipid, plastic and FT chemistry.

The dominance of MOF derived materials (17 of 29 studies) has an important implication: in most of the corpus, the final catalyst no longer contains a framework. The benefit attributed to the MOF therefore lies in its value as a synthetic template (metal loading and dispersion, carbon shell, porosity, heteroatom doping). Only a few studies compared the MOF derived catalyst directly with a conventionally prepared analogue at equal metal loading; notable exceptions are the Ni–BTC@MCM–41 versus impregnated Ni/MCM–41 comparison [18] and the comparisons with Pd/C [24], [25]. Without such controls, the claim that a MOF route is superior to cheaper impregnation or co precipitation routes remains partly untested. A related concern applies to "pristine" MOFs used at 390–440 °C [6], [18], most carboxylate frameworks are unlikely to survive such conditions intact, so post reaction structural characterisation is needed to establish whether the active phase is the MOF or a species formed from it in situ.

Table 2. Catalyst design strategies identified across the reviewed studies, with representative references, reported benefits and open questions.

Design strategy	Principle	Ref.	Reported benefit	Risks/open questions
Defect engineering of Zr–MOFs	Modulators create missing linker/missing cluster defects; more accessible μ_3–OH / Zr sites and secondary mesoporosity	1], [10], [15]	Conversion and selectivity to C_{11}–C_{12} adducts up to ≈100%	Fouling by furfural derived deposits; framework cannot be regenerated by calcination
Dispersion on mesoporous supports	MOF nanodomains grown on MCM–41/SBA–15 or zeolites; better accessibility and dispersion	[9], [14], [18]	≈2× (MOF–808/MCM–41) to ≈20× (UiO–66@SBA–15) higher conversion than bulk MOF; 75% less Ni (Ni–BTC@MCM–41)	Lower MOF loading; stability gains still limited to ≈3 cycles
Linker functionalisation and guest encapsulation	–SO_3H, –OH or amine groups; heteropolyacids or POMs confined in cages	[3], [6], [11], [22]	Tunable Brønsted/Lewis acidity; shape selectivity; water tolerance	Cr–based frameworks; leaching risk of guests; thermal limits
Pyrolysis to metal/carbon or metal/oxide	Linker carbonises; metal forms small, anchored nanoparticles (Ni, Co, Ni_2P)	[2], [8], [19], [24]	High dispersion and metal loading; stable at 300–460 °C	Framework is lost; seldom benchmarked against impregnated analogues
Multimetallic and heteroatom doped precursors	Co–/ion exchange before pyrolysis; electron transfer, O vacancies, spillover	[4], [23], [25], [28], [29]	Enhanced C–O and C–C cleavage; noble metal free hydrogenation	Complex synthesis; active site attribution uncertain
Spatially separated tandem catalysis	Acid MOF and hydrogenation catalyst as separate particles; adsorption expulsion of intermediates	[3]	Single component alkanes; modular, recoverable	Relies on noble metal (Pd/C); integrated control not tested in same study
Integrated bifunctional (assembly line) catalysts	Base + acid/metal sites in one solid or MOF derived metal + zeolite	[7], [16]	One–pot C–C coupling + HDO; C_8–C_{16} beyond ASF limit	Coke and carbon loss; limited reuse data

3.2. Site engineering: defects, acid base balance and electronic effects

Three design principles recur across routes. First, defect engineering increases the number and accessibility of active sites: modulator pK_a controls the balance between missing linker defects (which alter acid character) and missing cluster defects (which open mesopores), and combining both gave the most active UiO–66 catalysts [15]. Second, the type and strength of acid or base sites must match the reaction: only Cs derived strong bases activated the α–H of MIBK [13]; increasing Lewis acidity through pyrolysis improved FAME deoxygenation [8]; and in the one–pot aldol–HDO system, amine bases and phosphide–derived acid sites operated together [16]. Third, multimetallic MOF precursors enable electronic tuning that is difficult by impregnation, including electron transfer in Co–Mo–Ni with associated oxygen vacancies [4], Ni–Co and Mo–Co heterointerfaces for phenol HDO [12], [28], Pt–Ni synergy lowering NiO_x reduction temperature [20], La promotion of Ni dispersion and acidity [23], and Ru promotion of Co reducibility [29]. Hydrogen spillover at Ni/support interfaces is a further lever that can substitute for noble metals in terpene hydrogenation [25].

3.3. Proximity versus separation of catalytic functions

A conventional principle of bifunctional catalyst design is that metal and acid sites should be close together. The corpus provides evidence both for and against this principle, depending on the reaction. For the precise HDO of cyclic ethers, separating the acid MOF and the Pd/C hydrogenation catalyst as distinct particles was beneficial, because olefinic intermediates were expelled from the acidic pores and hydrogenated elsewhere before they could oligomerise or isomerise, and because Pd was protected from strong acid [3]. Liu et al. noted that Pd supported directly on MIL–101–SO_3H had been reported elsewhere to be incompatible with HDO conditions, but did not test such a catalyst themselves; a direct, same study comparison of integrated versus mechanically mixed configurations is therefore still missing. Conversely, for the one–pot aldol–HDO of furfural, an integrated Ni_2P@C–E catalyst outperformed a physical mixture of its components (86% versus 73%) [16], and in FT synthesis the "assembly line" combination of a Co phase and ZSM–5 achieved the highest SAF selectivity [7]. The appropriate distance between functions is therefore reaction specific: separation is favoured when reactive intermediates are prone to acid catalysed side reactions and can diffuse readily between particles, whereas proximity is favoured when intermediates are strongly adsorbed or easily lost as coke.

3.4. Stability, water and fouling

Water is formed in almost every deoxygenation and condensation reaction, and several studies turned this apparent weakness into a design parameter. Hydrophobic octyl grafting protected Cs/ZrO_2–C from water produced during the reaction [13], and adsorbed water on MIL–101–SO_3H added Brønsted acidity rather than destroying it [3]. Fouling by strongly adsorbed organics, rather than framework collapse, was the dominant cause of deactivation in furanic condensation [1], [10], [14], and it was mitigated by lowering the FUR/catalyst ratio, dispersing the MOF on silica or switching to continuous flow. Regeneration is a specific difficulty for intact MOFs, because the calcination normally used to burn off coke is incompatible with frameworks that decompose above ~200 °C [5]. For MOF–derived catalysts, the reported durability ranges from excellent (ten cycles for Ni@C/rGO [24]; 192 h on stream in FT synthesis [29]) to poor (a >40% relative loss in hydrocarbon yield within three runs with coconut oil [2]).

The most serious gap, however, is the absence of stability data. Ten of the 29 studies, including seven of the ten lipid studies and both municipal plastic studies, reported no reuse or time on stream data at all. Only three studies reported continuous operation longer than 50 h [5], [7], [29], and none tested a MOF catalyst for more than 200 h.

3.5. Comparability of the reported performance

Head–line values from different studies cannot be compared directly, for five reasons. *(i) Metric basis.* Results were reported variously as conversion, selectivity, isolated yield, GC calibrated yield, relative GC-MS peak area or response surface predictions; "jet selectivity" based on peak areas [12], [22] is not a mass yield. *(ii) Catalyst to feed ratio.* Ratios ranged from 1:200 [19] to 20:1 [28], a span of more than three orders of magnitude, and high ratios such as 1:1 [17] or 5:1 [12] can hide low intrinsic activity. Few studies reported turnover frequencies or space–time yields. *(iii) Scale.* Several results were obtained with milligram feed quantities in analytical micro reactors [12], [28], whereas preparative scale demonstrations were limited to 10 g [3]. *(iv) Feedstock realism.* Only 12 of the 29 studies used a real or waste derived feedstock (for example microalgal biodiesel or lipids, coconut oil, waste cooking oil, eucalyptus oil, heavy turpentine, polycarbonate waste or municipal plastics); the rest used reagent grade model compounds, and no study examined the effect of sulfur, nitrogen, chlorine or metal impurities on a MOF catalyst. (v) *Fuel quality.* Fuel properties were reported in only a few studies, such as higher heating value and density [18], density, heat of combustion,

freezing and flash points [24], or selected physical properties [21], [26]. No study evaluated the full set of jet–fuel specification properties required for SAF qualification (e.g. under ASTM D7566/D1655), and none reported a techno economic or life cycle assessment; the only process level analysis was a simulation of product separation [23].

4. Future directions

The studies reviewed here establish proof of concept across five SAF routes, but several steps are needed before MOF catalysts can be taken seriously for production. *(i) Standardised reporting.* Studies should report mass based product yields with carbon balances, the carbon number distribution within C_8–C_{16}, catalyst to feed ratio and space velocity, turnover frequency or productivity per unit metal, and the analytical basis of every value (calibrated GC FID versus GC MS area). A minimal common data set would allow meta analysis, which is not possible with the present corpus. *(ii) Durability under realistic conditions.* Stability testing should move from three to five batch cycles to continuous operation of hundreds of hours, including regeneration protocols compatible with the framework or its derivative. Post reaction characterisation (XRD, porosimetry, metal leaching by ICP) should be routine, particularly for intact MOFs operated at ≥300 °C. *(iii) Real feedstocks and impurities.* Lipid studies should progress from methyl palmitate to crude or waste oils containing free fatty acids, phospholipids, sulfur and nitrogen; furanic studies should use crude furfural streams; and plastic studies should assess chlorine from PVC and additives. The water tolerance demonstrated for MIL–101–SO_3H and hydrophobised Zr based catalysts should be tested with realistic water contents. *(iv) Fair benchmarks.* Each MOF derived catalyst should be compared with a conventionally prepared catalyst of the same composition and metal loading, and with a commercial benchmark (e.g. Pd/C, NiMo/Al_2O_3, Pt/zeolite), so that the added value of the MOF route can be quantified against its higher synthesis cost. *(v) Integration towards finished fuels.* Most furanic studies stop at oxygenated precursors, and most lipid studies stop at mixtures of alkanes and aromatics. One–pot or cascade processes [3], [16] and bifunctional designs [7] point the way, but products need to be evaluated against jet fuel specifications, including freezing point, density, aromatic content, thermal stability and lubricity, preferably in blends. *(vi) Scalability and sustainability.* The corpus contains no techno–economic or life cycle assessment. Scalable, solvent lean MOF synthesis (aqueous routes such as the Ni–MOF–74/GO method [24]), shaping into extrudates or supported forms [5], [14], replacement of noble metals by Ni and Co, and the avoidance of toxic metals such as Cr [3], [22] should be assessed quantitatively alongside catalytic performance.

5. Conclusion

This mini review mapped 29 experimental studies (2017–2026) that used MOFs or MOF–derived materials to convert biomass platform molecules, lipids, terpenes, lignin models, waste plastics and syngas into SAF–range hydrocarbons or their precursors. MOF derived catalysts, mainly Ni and Co based nanoparticles in carbon or oxide matrices, dominate the field and have been used for high temperature deoxygenation, cracking, plastic upcycling and Fischer Tropsch synthesis, whereas intact Zr– and Cr–based MOFs have been used mainly for lower temperature acid and base catalysed C–C coupling and precise HDO. Defect engineering, dispersion on mesoporous supports, linker functionalisation and multimetallic precursors emerge as the main design levers, and the optimal distance between metal and acid functions is reaction specific rather than universal. Best case laboratory performance is high, with near complete conversion and selectivity for aldol adducts, 70–84% jet range selectivity from FAMEs, up to 98% alkane yields in precise HDO and 75% C_8–C_{16} selectivity in Fischer Tropsch synthesis. However, the evidence base remains shallow: a third of the studies reported no stability data, most used model compounds, performance metrics are not comparable across studies, and none evaluated full fuel specifications, cost or life cycle impacts. Closing these gaps, rather than reporting further incremental gains in selectivity, is now the main requirement for establishing whether MOF catalysis can contribute to SAF production.

Declaration of generative AI use

During the preparation of this manuscript, the authors used Claude to improve the language, grammar, and overall readability of the manuscript. Gemini NotebookLM was used to assist with the design and visual presentation of figures. The authors reviewed, edited, and verified all AI assisted content and take full responsibility for the accuracy, originality, and integrity of the final manuscript.

References

[1] M. Sanz, D. de la Calle, J. Cueto, A. Martin, G. Morales, J. A. Melero, and M. Paniagua, "Selective production of cycloalkane SAF precursors from furfural and ketones over defective UiO–66(Zr) catalyst," *Fuel*, vol. 422, p. 139189, 2026, doi: 10.1016/j.fuel.2026.139189.

[2] A. Nugroho, P. D. C. Dewi, Sudiyarmanto, L. N. Hidayati, A. Kristiani, F. Aulia, A. N. Bakti, J. Prasetyo, N. Rinaldi, and D. Dahnum, "Catalytic deoxygenation of coconut oil to bio–jet fuel range hydrocarbon over nickel on ZIF–67–derived metal oxide," *Fuel*, vol. 407, p. 137430, 2026, doi: 10.1016/j.fuel.2025.137430.

[3] D.–H. Liu, H.–L. He, J.–J. Wang, S.–Y. Zhou, T. Zeng, X.–Y. Gao, Y. Xiao, X. Yi, A. Zheng, Y.–B. Zhang, and Z. Li, "Acidic metal–organic framework empowered precise hydrodeoxygenation of bio–based furan compounds and cyclic ethers for sustainable fuels," *Green Chemistry.*, vol. 23, no. 24, pp. 9974–9981, 2021, doi: 10.1039/d1gc03055h.

[4] Y. Qi, J. Cheng, M. Zhao, and Y. Mao, "Trimetallic Co–Mo–Ni catalyst derived from layered metal–organic frameworks for efficient bio–jet fuel production," *Applied Catalysis B: Environment and Energy*, vol. 383, p. 126057, 2026, doi: 10.1016/j.apcatb.2025.126057.

[5] K. Dussan, M. Peters, S. M. Scalzullo, B. Smith, A. van Zomeren, X. Baucherel, A. Kraft, and J. W. van Hal, "Catalytic condensation of biobased molecules for jet fuel synthesis," in *Proceeding 31st European Biomass Conference and. Exhibition*, Bologna, Italy, June 5–8, 2023.

[6] J. Cheng, Y. Shao, H. Guo, Z. Zhang, Y. Mao, L. Qian, K. Xin, and W. Yang, "Ni–based metal–organic frameworks prepared with terephthalic acid hydroxylation converted methyl palmitate into jet–fuel range hydrocarbons in CO2 atmosphere," *Fuel*, vol. 318, p. 123679, 2022, doi: 10.1016/j.fuel.2022.123679.

[7] G. Chen, Z. Ma, W. Gu, P. Liu, T. Lan, and Y. Lu, "Uniform silica–infused ZIF–67 derived Fischer−Tropsch cobalt catalyst integrated with ZSM–5 for sustainable aviation fuel synthesis," *Chemical Engineering Journal*, vol. 532, p. 174364, 2026, doi: 10.1016/j.cej.2026.174364.

[8] Y. Mao, J. Cheng, Y. Shao, H. Guo, L. Qian, and W. Yang, "Highly active Ni nanocatalysts derived from metal–organic framework (Ni–BDC) boosted deoxygenation and cracking of fatty acid methyl esters," *Industrial and Engineering Chemistry Research*, vol. 62, no. 32, pp. 12491–12500, 2023, doi: 10.1021/acs.iecr.3c01463.

[9] M. Sanz, P. Leo, M. Paniagua, J. A. Melero, and G. Morales, "Zr–based metal–organic frameworks and SBA–15 silica support: a synergistic approach for bio–jet fuel precursors production," *Biofuel Research Journal*, vol. 50, pp. 2684–2697, 2026, doi: 10.18331/BRJ2026.13.2.3.

[10] D. de la Flor, C. López–Aguado, M. Paniagua, G. Morales, R. Mariscal, and J. A. Melero, "Defective UiO–66(Zr) as an efficient catalyst for the synthesis of bio jet–fuel precursors via aldol condensation of furfural and MIBK," *Journal of Catalysis*, vol. 401, pp. 27–39, 2021, doi: 10.1016/j.jcat.2021.07.006.

[11] R. S. Malkar, H. Daly, C. Hardacre, and G. D. Yadav, "Aldol condensation of 5–hydroxymethylfurfural to fuel precursor over novel aluminum exchanged–DTP@ZIF–8," *ACS Sustainable Chemistry and Engineering*, vol. 7, no. 19, pp. 16215–16224, 2019, doi: 10.1021/acssuschemeng.9b02939.

[12] Y. Zhang, J. Jiang, J. Wu, M. Wen, and J. Wang, "Upcycling waste polycarbonate plastics into jet fuels over NiCo/C by catalytic tandem hydropyrolysis/hydrodeoxygenation," *Fuel Processing Technology*, vol. 247, p. 107809, 2023, doi: 10.1016/j.fuproc.2023.107809.

[13] Y. Zhao, M. Fan, P. Wang, C. Li, L. Wang, and L. Wang, "Hydrophobic strong solid base derived from graphene oxide hybrid zirconium MOFs and its enhanced stability on furfural–MIBK aldol condensation to synthesize branched biofuel precursors," *Fuel Processing Technology*, vol. 198, p. 106250, 2020, doi: 10.1016/j.fuproc.2019.106250.

[14] G. Morales, M. Paniagua, D. de la Flor, M. Sanz, P. Leo, C. López–Aguado, H. Hernando, S. A. Orr, K. Wilson, A. F. Lee, and J. A. Melero, "Aldol condensation of furfural and methyl isobutyl ketone over Zr–MOF–808/silica hybrid catalysts," *Fuel*, vol. 339, p. 127465, 2023, doi: 10.1016/j.fuel.2023.127465.

[15] M. Sanz, P. Leo, C. Palomino, M. Paniagua, G. Morales, and J. A. Melero, "Boosting the activity of UiO–66(Zr) by defect engineering: efficient aldol condensation of furfural and MIBK for the production of bio jet–fuel precursors," *Green Chemistry*, vol. 26, no. 13, pp. 7337–7350, 2024, doi: 10.1039/d3gc05022j.

[16] S. Yin, Y. Zhang, X. Tang, L. Dai, and Y. Wang, "Preparation of metal–organic framework–derived bifunctional catalysts for efficient one–pot synthesis of bio–jet fuel," *Bioresource Technology*, vol. 462, p. 135576, 2026, doi: 10.1016/j.biortech.2026.135576.

[17] L. Yang and M. A. Carreon, "Deoxygenation of palmitic and lauric acids over Pt/ZIF–67 membrane/zeolite 5A bead catalysts," *ACS Applied Material Interfaces*, vol. 9, no. 37, pp. 31993–32000, 2017, doi: 10.1021/acsami.7b11638.

[18] Y. Zhu, Z. Zhang, J. Cheng, H. Guo, and W. Yang, "Ni–BTC metal–organic framework loaded on MCM–41 to promote hydrodeoxygenation and hydrocracking in jet biofuel production," *International Journal Hydrogen Energy*, vol. 46, no. 5, pp. 3898–3908, 2021, doi: 10.1016/j.ijhydene.2020.10.216.

[19] Y. Xu, H. Guo, Y. Mao, L. Qian, W. Yang, and J. Cheng, "Modified Ni–based metal–organic frameworks (Ni–BTC) with high deoxygenation and cracking ability for production of a jet fuel–range hydrocarbon blend at a low catalyst dosage," *Industrial and Engineering Chemistry Research*, vol. 63, no. 25, pp. 11365–11373, 2024, doi: 10.1021/acs.iecr.4c00696.

[20] M. Wang, X. Shi, K. Wang, and H. Yuan, "Bimetallic hierarchical nanostructured alumina material catalyzes decarboxylation of oleic acid to produce long–chain alkanes for bioaviation kerosene," E*nergy Fuels*, vol. 38, no. 8, pp. 6992–7004, 2024, doi: 10.1021/acs.energyfuels.3c05227.

[21] T. Widjaja, A. Altway, S. Khoirunnisa, D. A. Nurhanifa, M. Mahfud, H. Juwono, J. Prasetyo, D. Dahnum, and A. A. Z. Rohmah, "Biofuel production from waste cooking oil over copper–metal–organic framework/potassium oxide catalyst for alternative bioenergy," *International Journal of Technology*, vol. 17, no. 2, pp. 376–394, 2026, doi: 10.14716/ijtech.v17i2.8009.

[22] S. Thakur, A. Bali, and K. N. Yogalakshmi, "Direct hydrodeoxygenation (HDO) of microalgal lipids into long–chain linear alkanes by peroxopolyoxotungstate (PPOM) incorporated MIL–100(Cr) catalyst," *Sustainable Chemistry One World*, vol. 11, p. 100272, 2026, doi: 10.1016/j.scowo.2026.100272.

[23] C. Chen, P. Liu, M. Zhou, J. Li, H. Xia, and J. Jiang, "One–step catalytic hydrotreatment of lignin dimer model compounds to cycloalkane and cycloalcohol by spherical metal–organic framework derived NiLa bimetallic materials," *Journal of the Energy Institute*, vol. 99, pp. 105–119, 2021, doi: 10.1016/j.joei.2021.08.012.

[24] X. Tang, Y. Yang, Y. Tang, S. Luo, X. Chen, X. Wei, and L. Wang, "Efficient hydrogenation of heavy turpentine into high–energy–density biofuel over MOF–derived nano–Ni@C/rGO and associated kinetic insights," *Journal of Environmental Chemical Engineering*, vol. 14, p. 121919, 2026, doi: 10.1016/j.jece.2026.121919.

[25] C. Wu, J. Fan, H. Mo, X. Chen, J. Liang, and L. Wang, "Engineering interfacial hydrogen spillover in Ni–decorated graphitic carbon nitride for solvent–free stereoselective hydrogenation of biomass α–pinene into cis–pinane for sustainable aviation fuel applications," *Applied Catalysis B: Environment and Energy*, vol. 386, p. 126377, 2026, doi: 10.1016/j.apcatb.2025.126377.

[26] S. A. H. Seyed Mousavi, S. M. Sadrameli, and A. H. Saeedi Dehaghani, "Catalytic pyrolysis of municipal plastic waste over nano MIL–53 (Cu) derived @ zeolite Y for gasoline, jet fuel, and diesel range fuel production," Process Saf. Environ. Prot., vol. 164, pp. 449–467, 2022, doi: 10.1016/j.psep.2022.06.018.

[27] S. A. H. Seyed Mousavi and A. H. Saeedi Dehaghani, "Catalytic pyrolysis of plastic waste to gasoline, jet fuel and diesel with nano MOF derived–loaded Y zeolite: evaluation of temperature, zeolite crystallization and catalyst loading effects," *Energy Conversion and Management*, vol. 299, p. 117825, 2024, doi: 10.1016/j.enconman.2023.117825.

[28] Y. Zhang, J. Wang, and J. Jiang, "Efficient polycarbonate plastic upcycling into jet fuel cycloalkanes over a bifunctional MoCo/NiC hetero–catalyst," *Chemical Engineering Journal*, vol. 500, p. 156733, 2024, doi: 10.1016/j.cej.2024.156733.

[29] M. Safari, A. Haghtalab, and F. Arabpour Roghabadi, "Promoting jet fuel production by utilizing a Ru–doped Co–based catalyst of Ru–Co@C(Z–d)@Void@CeO2 in Fischer Tropsch synthesis," *RSC Advances*, vol. 13, no. 49, pp. 35525–35536, 2023, doi: 10.1039/d3ra06624j.